Received: 13 May 2020 | Revised: 29 July 2020 | Accepted: 10 August 2020

DOI: 10.1002/mgg3.1490

Molecular Genetics & Genomic Medicine Open Access WILEY

ORIGINAL ARTICLE

A putative frameshift variant in the *CHM* gene is associated with an unexpected splicing alteration in a choroideremia patient

Tiziana Fioretti[1] | **Silvana Ungari**[2] | **Maria Savarese**[1] | **Fabio Cattaneo**[3] | **Enza Pirozzi**[4] | **Gabriella Esposito**[1,3]

[1]CEINGE - Advanced Biotechnologies, Naples, Italy

[2]Dipartimento di Scienze della Sanità Pubblica e Pediatriche, Azienda Ospedaliera S. Croce e Carle, Cuneo, Italy

[3]Department of Molecular Medicine and Medical Biotechnologies, University of Naples Federico II, Naples, Italy

[4]Azienda Ospedaliera S. Croce e Carle, Cuneo, Italy

Correspondence
Gabriella Esposito, Department of Molecular Medicine and Medical Biotechnologies, University of Naples Federico II, Via Pansini 5, 80131 Naples, Italy.
Email: gabriella.esposito@unina.it

Abstract

Background: Due to the limited availability of mRNA analysis data, the number of exonic variants resulting in splicing impairment is underestimated although aberrant splicing correction is a promising therapeutic option to treat monogenic diseases, including choroideremia (CHM), a rare X-linked eye disorder arising from sequence alteration of the *CHM* gene. Herein we report an exonic frameshift variant associated with an mRNA splicing alteration that leads to a *CHM* hypomorphic allele.

Methods: Total RNA and genomic DNA were extracted from peripheral blood of a patient affected by a mild form of CHM. The *CHM* gene was analyzed by PCR-based methods and Sanger sequencing.

Results: Besides the known c.1335dup frameshift variant, mRNA analysis revealed a splicing alteration that restored the reading frame of the mutant transcript, likely leading to an aberrant protein with residual activity. Bioinformatic analyses identified novel putative exonic splicing enhancer elements and provided clues that also pre-mRNA secondary structure should be taken into account when exploring splicing mechanisms.

Conclusion: A careful molecular characterization of the c.1335dup variant's effect explains the relationship between genotype and phenotype severity in a CHM patient and provides new perspectives for the study of therapeutic strategies based on splicing correction in human diseases.

KEYWORDS

choroideremia, exonic splicing enhancer, exonic variant, genotype-phenotype correlation, pre-mRNA structure, splicing

1 | INTRODUCTION

Choroideremia (CHM, OMIM: 303100) is an X-linked recessive eye disease characterized by slow degeneration of the choroid, photoreceptors and retinal pigmented epithelium (RPE). Its prevalence is estimated at 1 in 50,000 people of European descent. Affected males develop night blindness in their teenage years, which is followed by gradual loss of peripheral vision and later of central visual acuity, resulting in a significant vision loss at middle age (Coussa, Kim, &

Traboulsi, 2012; Di Iorio, Esposito, et al., 2019; Mitsios, Dubis, & Moosajee, 2018). Carrier females are generally asymptomatic, but funduscopic examination often shows areas of chorioretinal atrophy that represent clonal areas of the disease (Jauregui et el., 2019; Murro et al., 2017). Currently, there are no approved treatments available for patients affected by CHM. However, due to the relatively low progression, various therapeutic options including gene therapy, pharmacological compounds, non-viral gene delivery, and mutation-specific treatments are under study (Garanto, van der Velde-Visser, Cremers, & Collin, 2018; Trapani & Auricchio, 2019).

CHM is caused by pathogenic sequence variants in the *CHM* gene (MIM: 300390), on chromosome Xq21.2 (Dimopoulos, Radziwon, St Laurent, & MacDonald, 2017), which has 15 exons and encodes the ubiquitously expressed Rab Escort Protein 1 (REP1). REP1, like the closely related REP2 (MIM: 118825), is an essential component of the catalytic Rab geranyl-geranyl transferase II complex (Andres et al., 1993; Cremers, Armstrong, Seabra, Brown, & Goldstein, 1994) that catalyzes prenylation of the ras-related Rab GTPases, crucially involved in the regulation of intracellular membrane traffic (Ali & Seabra, 2005).

More than 330 unique *CHM* pathogenic variants, which realistically result in dysfunctional or absent REP1, are reported in public databases [Leiden Open Variant Database (LOVD), https://databases.lovd.nl/shared/genes/CHM; updated July 12, 2019; Human gene mutation database, HGMD®]. Mainly, CHM-causing variants are nonsense, splicing and frameshift base pair changes that often introduce a premature termination codon (PTC) in the mRNA; very rare are the missense variants, which presumably lead to low or no proteins expression. About 20% of CHM patients has chromosomal deletions of variable size that remove single/multiple exons or the whole *CHM* gene and various flanking genes (Esposito et al., 2011; Sanchez-Alcudia et al., 2016; Simunovic et al., 2016). Only in a few cases, large duplications, insertion of Alu or L1 repeated elements, or variants within the *CHM* promoter have been described, as well as an intronic variant that activates a cryptic exon (Andres et al., 1993; van den Hurk et al., 2003; Radziwon et al., 2017; Vaché et al., 2019; Zhou et al., 2017).

The molecular methodologies currently used to diagnose genetic diseases are mainly based on Sanger or next-generation sequencing of genomic DNA. A plethora of widely validated and frequently upgraded bioinformatic tools are freely available to assess pathogenicity of sequence variants. These programs are often able to predict whether sequence changes, also occurring in coding region, may cause splicing alteration. However, mRNA analysis and/or functional studies are very rarely performed and the actual consequence of the bulk of putative exonic splicing mutations on gene expression remains unverified in the most diverse genes (Di Iorio, Orrico, et al., 2019; Esposito et al., 2017). Identification of natural sequence variants that affect splicing through unusual molecular mechanisms of pre-mRNA processing regulation increases our knowledge on this topic and provides useful information to improve accuracy of currently available methods that predict the pathogenicity of genomic variants. Furthermore, elucidation of gene-specific mechanisms that control splicing is crucial especially considering that aberrant splicing correction is a novel promising therapeutic option to treat genetic diseases, including CHM (Garanto et al., 2018).

Herein we report the results of the molecular analysis performed in a male patient affected by choroideremia and their relationship with disease severity. We also examined *in silico* the molecular mechanisms that realistically explain how a typical frameshift variant in the *CHM* coding region causes an unexpected exon skipping that restores the mRNA reading frame.

2 | MATERIALS AND METHODS

2.1 | Ethical compliance

Informed consent was signed by the patients who approved to undergo the molecular analysis, which was performed for clinical diagnostic purposes according to the guidelines for genetic tests approved by the Italian Ministry of Health. By signing the informed consent, patients also agreed to the use of their clinical and molecular data for research scope and scientific publications, in anonymous form. Analysis was carried out in accordance with the Institutional Guidelines and with the Declaration of Helsinki.

2.2 | Patient description and clinical examination

Proband was a 50-year-old man who was diagnosed with CHM. His family history was notable for poor vision in a maternal uncle, deceased for stroke at the age of 57 years, thereby supporting the X-linked inheritance pattern. Patient's medical history was marked by nyctalopia and poor peripheral vision since childhood; he was affected by type 2 diabetes and coronary heart disease that was treated with angioplasty.

Optical coherence tomography (OCT), infrared confocal scanning laser ophthalmoscopy and fundus autofluorescence were performed with the SPECTRALIS® Multimodal Imaging platform (Heidelberg Engineering, Franklin, MA 02038, USA). Fundus autofluorescence imaging was obtained with infrared and blue light autofluorescence. The

vessels of the choroid were observed by fluorescein (FA) and indocyanine green (ICGA) angiography.

2.3 | Molecular analysis

Genomic DNA was extracted from peripheral blood leukocytes with the Nucleon™ BACC2 kit (GE Healthcare Italia, Milan, Italy). *CHM* exons (NG_009874.2; NM_000390.4) with their flanking regions were amplified by PCR, as reported elsewhere (Esposito et al., 2011). Total RNA was isolated from peripheral blood leukocytes using the QIAamp RNA blood mini kit (Italy-QIAGEN S.p.A., Milan, Italy). Five hundred nanograms of total RNA were reverse transcribed and subsequently amplified in three partially overlapping fragments (CHM1, exons 1–6; CHM2 exons 5–12; CHM3 exons 11–15), using the conditions provided with the one-step RT-PCR system (Invitrogen Italy s.r.l.) and primers (10 μM each) previously described (Beaufrere et al., 1997; Esposito et al., 2011).

2.4 | *In silico* study

Pathogenicity of the c.1335dup variant was assessed by MutationTaster (Schwarz, Cooper, Schuelke, & Seelow, 2014). Relevant splicing sequences in normal and mutant DNA sequence were analyzed using the webservers Human splicing finder v.3.1 (http://www.umd.be/HSF/, accessed May 2019) (Desmet et al., 2009) and ESEfinder v.3.0 (http://krainer01.cshl.edu/cgi-bin/tools/ESE3/esefinder.cgi?process=home, accessed on May 2019) (Cartegni, Wang, Zhu, Zhang, & Krainer, 2003). Protein and nucleotide sequence alignment of the *CHM* gene and of the *CHML* gene (MIM: 118825; NM_001821.3) were performed by BLAST (https://blast.ncbi.nlm.nih.gov/Blast.cgi). *In silico* analysis to investigate influence of the c.1335dup variant on pre-mRNA secondary structure was performed using the default modeling parameters of the webservers mFold (http://mfold.rit.albany.edu/?q5mfold, accessed on May 2019) (Zuker, 2003) and RNAfold (http://rna.tbi.univie.ac.at/cgi-bin/RNAWebSuite/RNAfold.cgi, accessed on May 2019) (Gruber, Bernhart, & Lorenz, 2015), which are both able to model secondary structures of single stranded RNA or DNA sequences.

3 | RESULTS

3.1 | Clinical findings and molecular study

Although proband experienced nyctalopia and poor peripheral vision since childhood, he acknowledged the risk to be affected by CHM about 3 years earlier, when he knew that a maternal uncle had the disease. Indeed, despite the proband being 47 years old, his visual acuity was normal in both eyes (RE = 10/10; LE = 10/10) without correction. However, when he performed fundus examination, the revealed typical areas of atrophy in the middle and extreme periphery of the RPE were consistent with CHM (Coussa et al., 2012; Di Iorio, Esposito, et al., 2019). Indeed, infrared confocal scanning laser ophthalmoscopy and fundus autofluorescence showed preserved foveal profile and crescent-shaped area of preservation in the macular region, within a framework of CHM due to a significant atrophy of the choroid (Coussa et al., 2012; Di Iorio, Esposito, et al., 2019) (Figure 1a–d). FA (Figure 1e,f) and ICGA (Figure 1g,h) showed prominent choroidal vasculature with partial choriocapillaris sparing in macula region. Also OCT angiography revealed relatively preserved deep retinal vasculature and residual flow in the choriocapillaris, which roughly corresponded to the autofluorescence areas seen in Figure 1c,d.

According to an *in house* validated diagnostic algorithm (Esposito et al., 2011), we started the molecular diagnosis of CHM in the proband by analyzing the *CHM* mRNA. The *CHM* gene is expressed in all human tissues; therefore, if a fresh blood sample is available, preliminary mRNA analysis is warranted, especially in male patients. Indeed, in a shorter time than DNA analysis, mRNA analysis may identify exonic variants, exon deletions/duplications and splicing alterations (Furgoch, Mewes-Arès, Radziwon, & Macdonald, 2014). Hence, in our proband, we amplified the *CHM* cDNA in three overlapping fragments, by one-step RT-PCR (Esposito et al., 2011). The amplification product spanning exons from 6 to 12 had a lower molecular mass than the corresponding normal fragment (Figure 2a) and was, therefore, analyzed by Sanger sequencing. Despite sequence quality was quite poor, we were able to clearly reveal that the cDNA fragment, consistently to its abnormal size, lacked the whole sequence encoding exon 11; in addition, we detected the duplication of adenine at position c.1335, located 15 nucleotides before the end of exon 10 (Figure 2b).

Therefore, we amplified and sequenced genomic regions corresponding to *CHM* exons 10, 11 and 12 and confirmed the presence of the c.1335dup variant in exon 10 (Figure 2c), whereas no sequence variants were identified in exons 11 and 12. Moreover, we sequenced intron 10 without detecting any variant. Notably, the c.1335dup segregated with the disease in the family because the proband's female cousin was heterozygous of this variant (Figure 2d).

The NM_000390:c.1335dup was reported in the literature as a pathogenic frameshift variant, without any data concerning its consequences on the mRNA structure (Simunovic et al., 2016). According to our usual procedure, we interrogated the bioinformatic tool MutationTaster that predicted this variant was pathogenic as consequence of a reading frame shift (p.Arg446 Thrfs*), but it also raised the possibility of a splicing

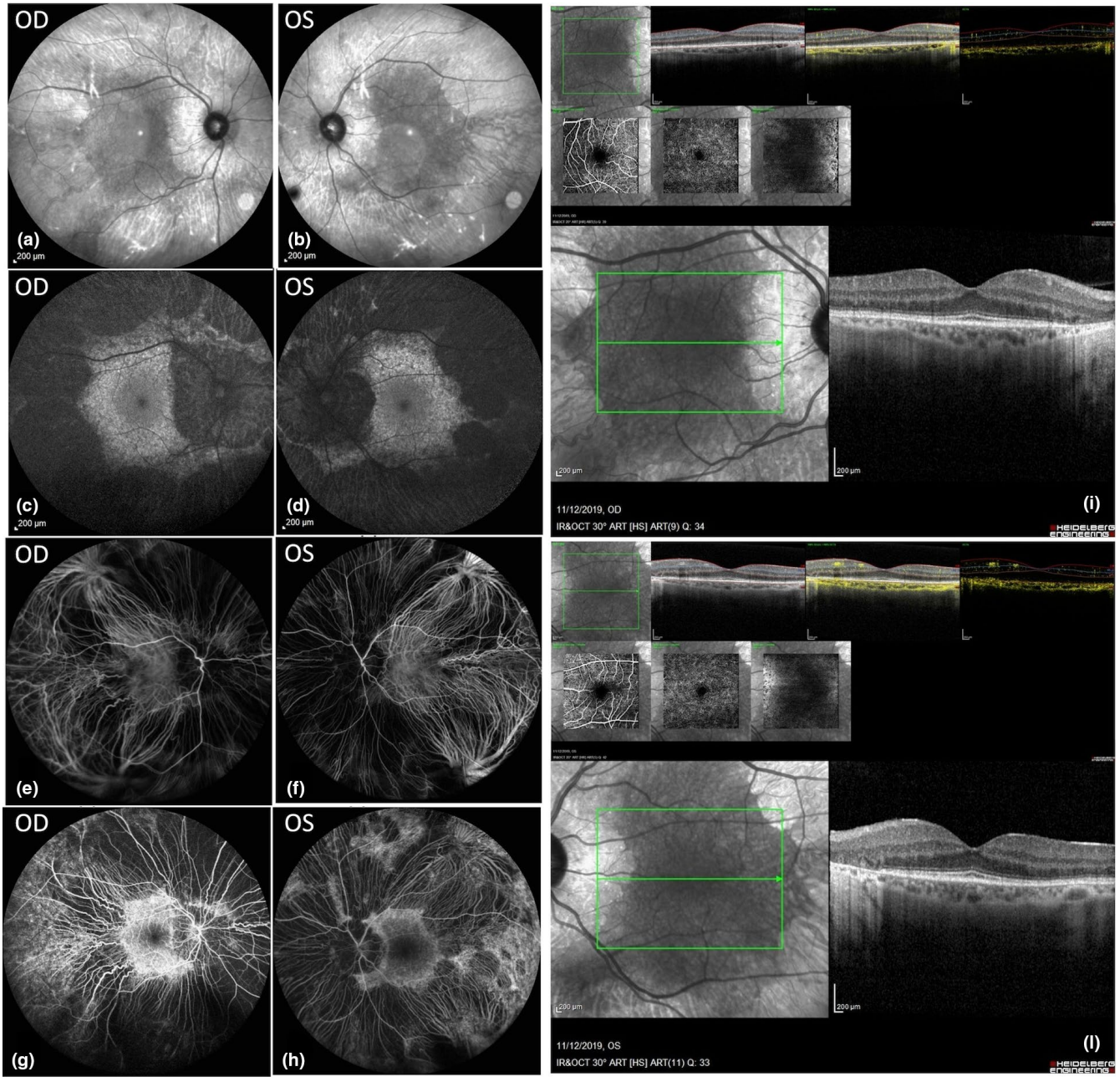

FIGURE 1 Retinal imaging of the proband. Heidelberg fundus autofluorescence (AF) imaging shows, in both the eyes, significant atrophy of the choroid sparing a wide residual central area of AF preserving macula, with either infrared (a and b) and blue light (c and d) AF. Fluorescein angiography (e and f) and indocyanine green angiography (g and h) reveal prominent choroidal vasculature and residual choriocapillaris corresponding to the areas of the "AF islands" seen in C and D. SD-OCT imaging of the right (i) and left (l) eye shows residual choriocapillaris, ellipsoid zone band and RPE. OD, right eye; OS, left eye

defect. Indeed, in our patient, this single nucleotide insertion was associated with the skipping of exon 11, which is 64 nucleotide long. As subtraction of 64 nucleotides and insertion of 1 nucleotide deprive the aberrant mRNA of a total of 63 nucleotides, we argued that exon 11 skipping restored the reading frame loss due to the c.1335dup. We, therefore, evaluated the putative effect of this complex mRNA aberration on REP1 structure using an on-line tool that was able to translate *in silico* a nucleotide sequence into a protein (https://web.expasy.org/translate/). The predicted mutated REP1 was shorter than the normal because it lacked the 21 amino acids encoded by exon 11, as revealed by protein BLAST alignment; moreover, the transient reading frame shift occurred immediately downstream the duplication site changed the four amino acids encoded by the last 15 (+1 dup) nucleotides of exon 10 (see Figure S1A). Despite the predicted huge modification in the REP1 structure, at 50 years of

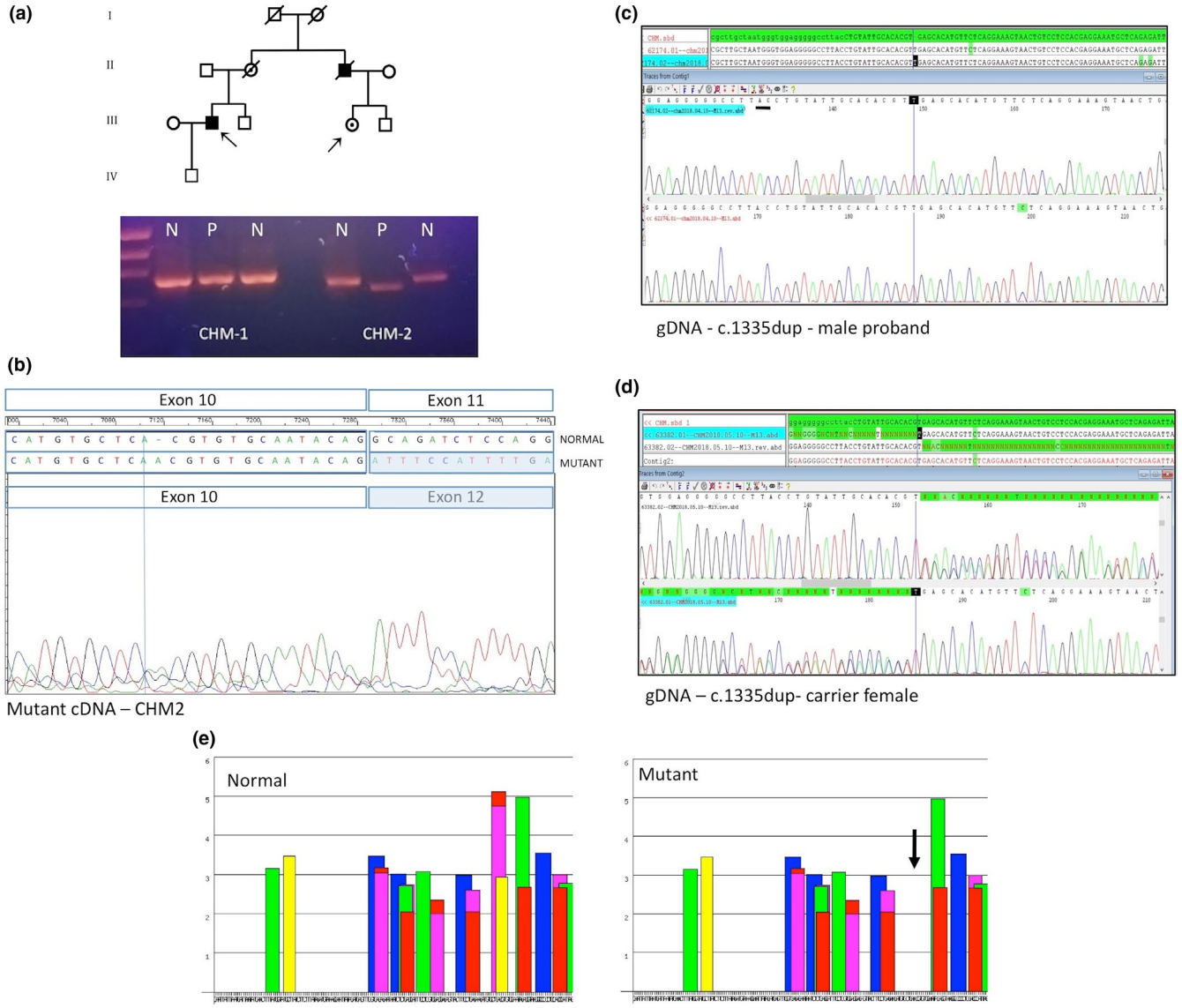

FIGURE 2 The c.1335dup variant in *CHM* exon 10 is associated with exon 11 skipping. (a–d) Molecular analysis of the *CHM* gene in the proband. (a) Agarose gel electrophoresis of cDNA fragments CHM-1 (left) and CHM-2 (right), obtained by RT-PCR in the proband (P) and in normal males (N). The CHM-2 fragment is smaller in the proband than in the controls. (b) Sequence electropherogram of the CHM-2 cDNA fragment reveals the c.1335dup and the skipping of exon 11, in the proband. Electropherograms of the genomic sequence of exon 10, (c) in the proband and (d) in his carrier female cousin. Both the electropherograms represent sequences of the reverse strand. (e) Predicted consequences of c.1335dup on the binding of auxiliary splicing factors to RNA. Screenshots of the ESEfinder 3.0 analysis (http://krainer01.cshl.edu/cgi-bin/tools/ESE3/esefinder.cgi?process=home) performed for the normal (left) and mutant (right) sequences of *CHM* exon 10. The binding sites of SRSF1 and SRSF6 (red/purple and blue bars, respectively) are lost in the mutant sequence (black arrow in the right panel)

age the patient still had normal visual acuity without correction, in agreement with the conserved foveal profile and with the wide area of preservation in macular region (Figure 1).

3.2 | *In silico* analysis

In introns of eukaryotic genes, consensus sequences at 5′-(donor) and 3′-splice site (acceptor) are crucial in exon definition, representing the binding sites of U1 snRNP and of the heterodimeric U2 snRNP auxiliary factor U2AF65/35, respectively, which are required for initiating spliceosome assembly (Daguenet, Dujardin, & Valcárcel, 2015; Matera & Wang, 2014). However, to recruit a functional spliceosome, these sites generally require auxiliary *cis*-elements known as exonic and intronic splicing enhancers (ESEs and ISEs, respectively) and exonic and intronic splicing silencers (ESSs and ISSs, respectively), which bind splicing regulatory proteins that act as activators in constitutive splicing and/or modulate alternative splicing, respectively.

TABLE 1 Position of canonical splicing sites within the 1080 nucleotide long *CHM* sequence stretch used for *in silico* analysis.

Motif Type	Motif Name	Normal nt position	Mutant nt position[a]	Length	Sequence
Human splicing site	acceptor (Intron 9)	212 ~ 213	212 ~ 213	2	ag
	donor (Intron 10)	319 ~ 320	320 ~ 321	2	gt
	acceptor (Intron 10)	691 ~ 692	692 ~ 693	2	ag
	donor (Intron 11)	757 ~ 758	758 ~ 759	2	gt

[a]The c.1335dup occurs at nt 303 of the sequence and shifts the mutated sequence of one nucleotide. The GenBank reference sequences of *CHM* are NG_009874.2; NM_000390.4.

Point mutations involving the consensus sequences and auxiliary *cis*-elements that regulate splicing can cause improper recognition of exon/intron borders and result in the formation of aberrant transcripts (Anna & Monika, 2018); nevertheless, also RNA secondary structure has a relevant influence on the pre-mRNA splicing process (Warf & Berglund, 2010).

Therefore, we performed *in silico* analyses to localize, within the *CHM* sequence, splicing regulatory motifs that could be involved in the mRNA rearrangement detected in our patient, using several freely available bioinformatic tools.

In particular, we analyzed a 1080 nucleotides long sequence stretch spanning intron 9, exon 10 (from nt 214 to 318, in this sequence), intron 10, exon 11 (from nt 693 to 756) and 323 nucleotides of intron 11, in the normal *CHM* (Figure S1B). In the mutated sequence, the single nucleotide duplication c.1335dup (localized at nt 304 of 1080) extends exon 10 to nucleotide 319 and shifts the position of exon 11 (from nt 694 to 757).

Human splicing finder analysis predicted that the c.1335dup variant activated a new exonic cryptic donor splice site and a new ESE; moreover, it disrupted 2 putative ESEs, representing binding sites for the serine/arginine-rich RNA splicing factors SF2/ASF, aka SRSF1 (consensus sequence CTCACGT), and SRSF6, aka SRp55 (consensus sequence CACGTG), also according to the ESE finder tool results (Figure 2e). All the predicted alterations should be expected to affect splicing of exon 10, because the c.1335dup is located within this exon. However, in the patient's mRNA, splicing of exon 10 occurred correctly.

Thus, we considered the possibility that the loss of exon 11 identity could also depend on improper use of its canonical splicing sites, as consequence of pre-mRNA structural alteration. In order to investigate *in silico* the impact of the c.1335dup on pre-mRNA secondary structure, we submitted to the RNAfold and mFold webservers the 1080 nucleotide-long sequence that covers the splice sites flanking exon 10 and exon 11 of the pre-mRNA. Table 1 reports precise positions of the canonical splice sites within the normal and mutant sequence stretch. RNAfold and mFold servers use algorithms estimating the minimum free energy (MFE) structure of a RNA molecule. MFE represents a thermodynamic energy measurement based on intramolecular aromatic stacking and hydrogen bond interactions (Gruber et al., 2015). A low MFE value is representative of a very stable structure (Wu & Maniatis, 1993). For a given fragment, the nucleotide sequence alone determines the MFE computation.

Secondary structures predicted by both the servers showed that the mutation causes huge modification in the overall pre-mRNA structure of the analyzed sequence (Figure S2). Thus, we focused our attention on the structural features of the consensus splice sites flanking exon 10 and exon 11, in the normal and mutant sequence.

In particular, both RNAfold- and mFold-predicted secondary structures of the acceptor (Figure S3) and donor (Figure S4) splice sites immediately adjacent to exon 10 were similar in the normal and mutant sequence. In contrast, the splice sites flanking exon 11 showed slight differences in the donor site only comparing normal and mutant structures generated by RNAfold (Figure 3a–d), whereas both the programs predicted significant structural differences for the acceptor AG site before exon 11 (Figure 3e–h). Moreover, focusing on the polypirimidine stretch within the acceptor consensus sequence, the polyU tract that likely represents the binding site of U2AF65 is closed in a stable double-strand in the mutated sequence, whereas it has a more opened and potentially accessible hairpin structure in the normal sequence (Figure 3e–h). Notably, binding of U2AF65/35 to the acceptor consensus sequences within a pre-mRNA is also assisted by the auxiliary protein SRSF1 (Long & Caceres, 2009; Wu & Maniatis, 1993).

4 | DISCUSSION

Splicing defects have a predominant role in the molecular pathogenesis of genetic diseases. However, while the basic principle of splicing is well understood, it is still very

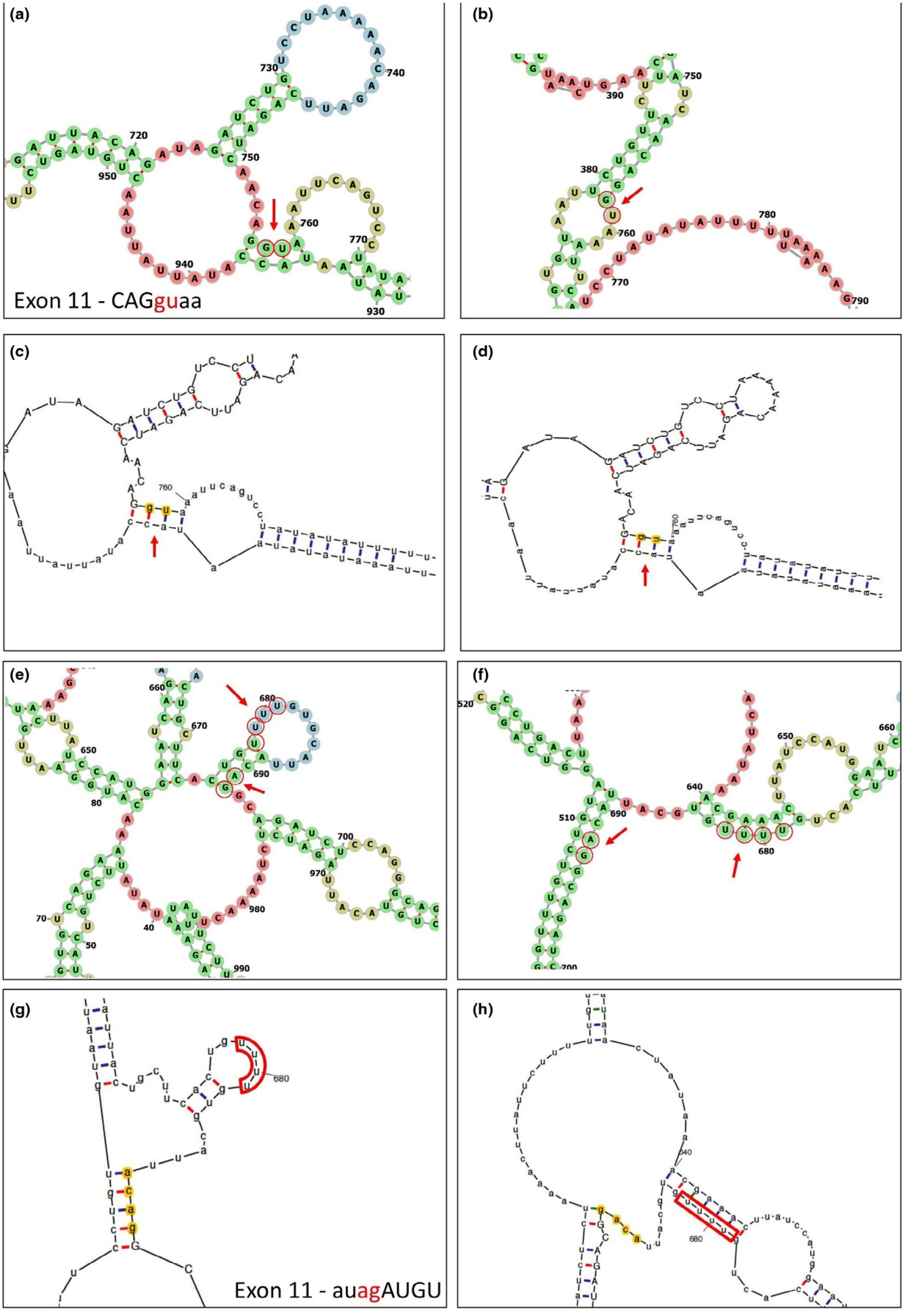

FIGURE 3 Structural details of the splice sites adjacent to exon 11. (a–d) Secondary structure of sequences including the donor GU dinucleotide (arrows) are different in the (a) normal (nt 757-758) and (b) mutant (nt 758-759) RNA, according to the prediction of RNAfold, whereas they are identical for the (c) normal and (d) mutant RNA, in the mFold prediction. In the RNAfold structures (a and b), nucleotides embedded in structure with different MFE are represented with different colors. The MFE content increases from green > yellow > cyan > pink; green structures have the most stable local conformations, with a more negative MFE value. (e–h) Secondary structure of the (e) normal RNA sequence including the acceptor AG dinucleotide (nt 691-692) significantly varies in comparison to the (f) mutant (nt 692-693), according to the prediction of RNAfold and mFold (g and h panels, for the normal and mutant structure, respectively). The whole consensus sequence, which includes the polypirimidine tract (circles in RNAfold, boxes in mFold structures) representing the putative binding site of U2AF65, spans nt 678-692 in the normal (e and g) and nt 679-693 in the mutant (f and h) pre-mRNA

difficult to predict splicing outcome. Therefore, identification of disease-associated DNA variants that affect splicing contributes to give new insights into molecular mechanisms of splicing regulation and to study novel strategies for splicing correction in human diseases, including CHM.

Numerous data indicate that, in human diseases, pathogenic sequence variants also distant from the canonical splice sites can affect, at RNA level, auxiliary splicing regulatory elements and interfere with exon recognition, thereby leading to exon skipping, or activate cryptic splice sites, resulting in partial exon deletion or in intron inclusion (Anna & Monika, 2018; Chabot & Shkreta, 2016). Moreover, correct splicing is finely regulated by other determinants, including pre-RNA structure and availability of specific splicing factors (Liu et al., 2010; Yadegari et al., 2016).

The *CHM* aberrant transcript expressed in the leukocytes of our patient had a single-nucleotide duplication localized 15 nucleotides upstream the end of exon 10 and was unexpectedly associated with the skipping of exon 11. In agreement with the Human Genome Variation Society recommendations for mutation nomenclature (den Dunnen et al., 2016), this complex mRNA sequence is described as *CHM*:r.[(1335dup;1350_1413del)]. No other mutation in the *CHM* gene coding and in intron 10 was detected, although a second intronic causative variation that impairs pre-mRNA splicing could not be excluded.

In silico analysis by MutationTaster predicted that the c.1335dup in the *CHM* gene was pathogenic as consequence of possible frameshift, non-sense mediated mRNA decay (NMD), amino acid sequence change, protein feature alteration, splice site change. Frameshift and splicing sequence variants are common cause of REP1 impaired expression in choroideremia patients (Dimopoulos et al., 2017; Furgoch et al., 2014; Sankila, Tolvanen, van den Hurk, Cremers, & de la Chapelle, 1992). Frameshifts usually lead to premature termination codon (PTC) and are associated with NMD of the aberrant mRNA or to the synthesis of truncated misfunctional/unstable proteins (Beaufrere et al., 1997; Esposito et al., 2011; Furgoch et al., 2014). Splicing mutations that affect canonical acceptor or donor dinucleotides often result in the skipping of the proximal exon in the mRNA, which ultimately causes frameshift with PTC or produces shorten misfunctional/unstable peptides. Interestingly, a synonymous *CHM* sequence variant (c.1359C>T; p.Ser453=) in exon 11 has been recently associated with exon 11 skipping (Sengillo et al., 2018), an mRNA alteration leading to a PTC (Esposito et al., 2011).

In the landscape of the *CHM* pathogenic variants, our finding that the frameshift c.1335dup is also a splicing variant associated with exon 11 skipping is very interesting. Indeed, coexistence of these two frameshift alterations restores the reading frame in the *CHM* aberrant transcript, thereby leading to the synthesis of a shorten protein with preserved carboxy-terminal end. Previous studies on REP1 structure indicated that C-terminus is essential for the maintenance of REP1 solubility and for membrane attachment (Rak, Pylypenko, Niculae, Goody, & Alexandrov, 2003). The evidence that the bulk of *CHM* pathogenic mutations causes loss of REP1 C-terminus further indicates that this protein domain is essential for the normal functioning of REP1 *in vivo* (Alory & Balch, 2001). On this basis, we speculate that the putative aberrant REP1 expressed in our patient, by retaining a residual functionality, may have contributed to preserve the patient's central vision at least up to the age of 50 years. Therefore, we can reasonably consider that the abovementioned reading frame repair ultimately transforms a potential null allele into a hypomorphic disease-allele, which mitigates the phenotype severity in our patient.

It is usually considered that disease-associated coding variants affecting splicing regulatory elements interfere with exon boundary identification and lead to exon skipping (Anna & Monika, 2018). Notably, the *CHM* exon 10 sequence, including the c.1335dup site, is preserved in the patient's mRNA. This implies that the c.1335dup variant does not impact accuracy of exon 10 splicing, despite bioinformatic analysis predicted it causes loss of ESEs in this exon. In contrast, the 64 nucleotides that form exon 11 are lost. In this regard, the genomic arrangement of the *CHM* gene supports an intriguing perspective. In fact, length of the 14 *CHM* introns ranges from 45681 to 374 nucleotides. Introns 9, 10, and 11, which flank the exons involved in the mRNA rearrangement, are 10072, 374 and 6361 nucleotide long, respectively. Intron 10, which is interposed between exons 10 and 11, is the shortest *CHM* intron; it is, therefore, conceivable that the putative ESEs disrupted in exon 10 by the c.1335dup are auxiliary for the correct splicing of the closely adjacent exon 11, rather

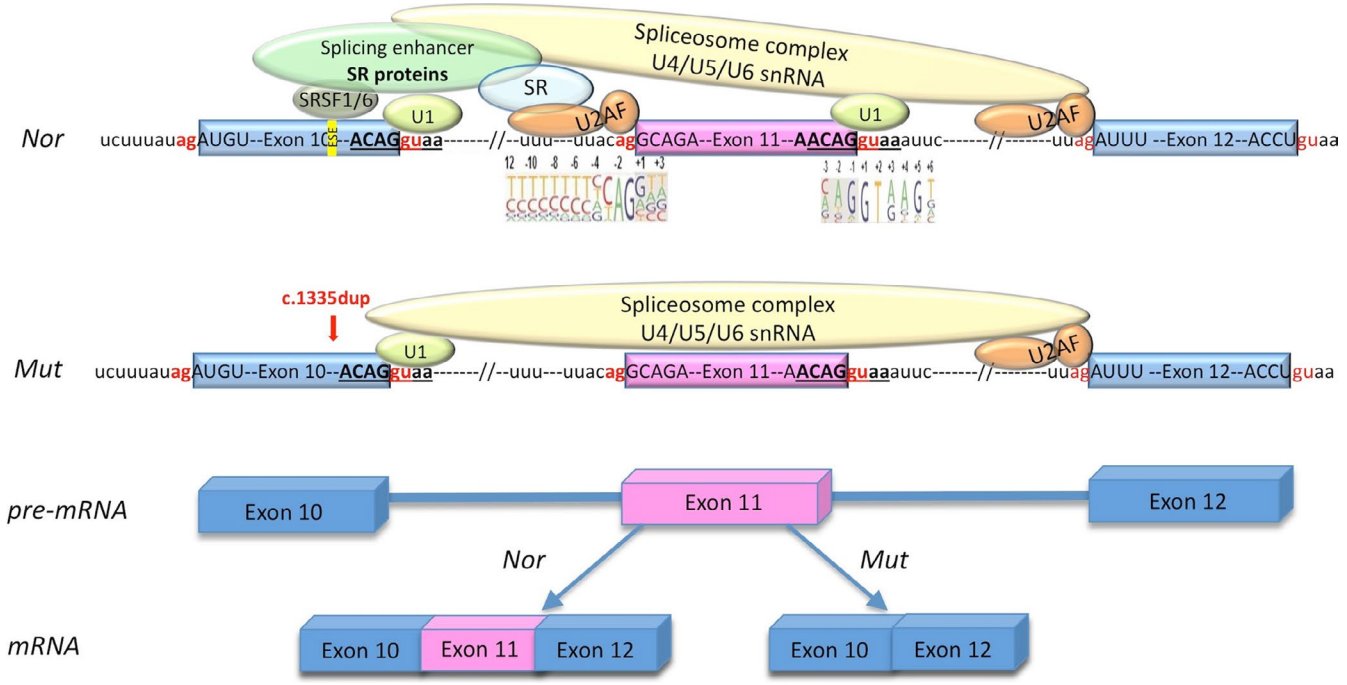

FIGURE 4 Model of the presumed c.1335dup-induced splicesome assembly modification leading to exon 11 skipping in the proband mRNA. Boxes represent the exons; key nucleotides of the splice sites are indicated, with the invariant 5′ GU and 3′ AG noted in red. In the normal pre-mRNA sequence (Nor), binding of splicing enhancer proteins including SRSF1/6 to the ESEs (small yellow box) in exon 10 triggers the recruitment of U2AF and U1, respectively, to the AG and GU dinucleotides flanking exon 11, thereby defining the identity of this exon that is, thus, included in the mRNA. In the mutant sequence (Mut), the c.1335dup (red arrow) abolishes these ESEs, SRSF1/6 are not loaded onto the mutant pre-mRNA at this site; as a result, exon 11 loses its identity and is skipped in the mRNA. The ACAGguaa sequence shared by the donor splice sites at the end of exons 10 and 11 is marked in bold and underlined

than of exon 10 itself (Figure 4). Indeed, these ESEs are putative RNA-binding domain of the serine/arginine-rich RNA splicing factor 1, SRSF1, which usually promotes exon inclusion, and of SRSF6, which is involved in alternative splicing regulation (Long & Caceres, 2009). It should be also noted that the canonical donor splice sequences (ACAGguaa) at the end of exons 10 and 11, respectively, are identical; it is, therefore, plausible they are both able to function as donors for the intron 11 acceptor site.

Interestingly, the *CHML* gene transcript (MIM: 118825), which encodes the REP2 isoform, shares 79.04% of sequence identity with *CHM*; in agreement, REP2 amino acid sequence has 72.38% of identity with that of REP1. Indeed, in CHM tissues other than eye, REP2 compensates for the REP1 deficiency. Notably, ^{445}SerArgVal^{447} of REP1 aligns to ^{447}SerAspVal^{449} of REP2; these amino acid stretches are encoded by the nucleotide sequences 5′–TCACGTGTG–3′ and 5′–TCAAATGTG–3′ of *CHM* and *CHML*, respectively, but only the first includes the putative binding sites (CACGTG) for the SRSF1/6 auxiliary factors. Because *CHML* is an intron-less gene, we speculate that such a strong element of splicing regulation is spared because it would not only be useless but could even be detrimental for the expression of this essential gene.

As sequence of the genomic regions corresponding to intron 10, exon 11 and exon 12 was normal in our patient, we also explored the possibility that the c.1335dup sequence variant influenced pre-mRNA splicing by other mechanisms. In particular, we considered the possible role of pre-mRNA structure in this aberrant mechanism of splicing.

Indeed, secondary structure of pre-mRNA molecules can have enhancing or inhibitory effects on splicing (Hamasaki-Katagiri et al., 2017; Liu et al., 2010). Negative examples of splicing include local structures around splice sites that decrease splicing efficiency and potentially cause mis-splicing. Consistently, transcripts of disease genes are significantly more structured around the splice sites and point mutations that affect the local structure often disrupt splicing (Soemedi et al., 2017).

According to the data obtained *in silico* by RNAfold and mFold analysis, the c.1335dup significantly alters the overall structure of the submitted pre-mRNA sequence. Very interestingly, the mutation does not alter significantly secondary structure of the canonical splice sites flanking exon 10 and consequently it does not affect their accessibility to specific or auxiliary splicing factors, in agreement to the correct splicing of this exon in the patient's mRNA. In contrast, the analysis evidences changes in the secondary

structure of the splicing site upstream exon 11 that can be compatible with the skipping of this exon. Indeed, in the mutant sequence predicted by RNAfold, the AG dinucleotide and the upstream polyU stretch are embedded in structured and stable double-strands, differently than the normal one; in addition, mFold creates a mutated structure that, while showing a more opened structure at the canonical AG in the mutant compared to the normal pre-mRNA, features a high stable double-stranded structure for the polyU tract upstream the 3′-end of intron 10. According to the model that increase of structure is a mechanism of splicing disruption, this stable structure sequesters the intronic polyU residues putatively involved in the interactions with U2SF65/35, which has a crucial role in exon identity definition.

In summary, the unusual splicing defect identified in the *CHM* mRNA of our patient with the c.1335dup may have occurred as result of the disruption of the ESEs that recruit SFSR1/SRSF6 and, despite they are located in exon 10, enhance splicing of the near exon 11, which shares the 3′ splicing sequences with exon 10 (Figure 4). Notably, these ESEs are absent in the homologous *CHML* gene, which shares about 80% of sequence identity with *CHM*, likely because they are detrimental for an intron-less gene. Exon 11 skipping can be fostered by the putative mutation-induced pre-mRNA structure alteration that masks relevant splicing sequences, thereby contributing to the exon 11 identity loss.

Our molecular findings emphasize the importance of mRNA analysis in determining the actual impact of *CHM* sequence variants on pre-mRNA processing. Therefore, also based on our previous indication that a more severe phenotype would appear in patients with absent *CHM* transcription (Di Iorio, Esposito, et al., 2019), systematic application of mRNA analysis to all CHM patients will be warranted, to explore further possible genotype–phenotype correlations (Fry et al., 2019).

In conclusion, our analysis focuses on a disease-mutation mechanism that provides intriguing insights into splicing regulatory mechanisms and in the relationship between genotype and phenotype, in CHM. Indeed, evidences that relevant RNA sequences and structures could be similarly targeted to modify the outcome of splicing events increase the possible applications to the use of small molecules that rationally target RNA and open new avenues for drug discovery in splicing-mediated disorders (Garcia-Lopez et al., 2018; Singh & Singh, 2018).

ACKNOWLEDGMENTS

The authors acknowledge the support from the staff of the molecular diagnostics laboratory of CEINGE—Advanced Biotechnologies for DNA analysis.

CONFLICTS OF INTEREST

The authors have no conflicts of interest to declare.

AUTHOR'S CONTRIBUTION

All authors made substantial contributions to the study and approved the final version of the manuscript. Below is the contribution of each author to the manuscript: Gabriella Esposito supervised the study, analyzed the overall data and drafted the original and revised version of the manuscript. Tiziana Fioretti and Maria Savarese were involved in the genetic and pathogenicity analyses and generated the figure showing results of the *CHM* gene molecular analysis. Tiziana Fioretti and Fabio Cattaneo performed *in silico* RNA analyses and contributed to generate the related figures and tables. Silvana Ungari and Enza Pirozzi performed the genetic and clinical characterization of the probands.

ORCID

Fabio Cattaneo https://orcid.org/0000-0002-5833-8333
Gabriella Esposito https://orcid.org/0000-0002-4255-7312

REFERENCES

Ali, B. R., & Seabra, M. C. (2005). Targeting of Rab GTPases to cellular membranes. *Biochemical Society Transactions*, *33*, 652–656. https://doi.org/10.1042/BST0330652

Alory, C., & Balch, W. E. (2001). Organization of the Rab-GDI/CHM superfamily: The functional basis for choroideremia disease. *Traffic*, *2*, 532–543. https://doi.org/10.1034/j.1600-0854.2001.20803.x

Andres, D. A., Seabra, M. C., Brown, M. S., Armstrong, S. A., Smeland, T. E., Cremers, F. P. M., & Goldstein, J. L. (1993). cDNA cloning of component A of Rab geranylgeranyl transferase and demonstration of its role as a Rab escort protein. *Cell*, *73*, 1091–1099. https://doi.org/10.1016/0092-8674(93)90639-8

Anna, A., & Monika, G. (2018). Splicing mutations in human genetic disorders: Examples, detection, and confirmation. *Journal of Applied Genetics*, *59*, 253–268. https://doi.org/10.1007/s13353-018-0444-7

Beaufrere, L., Tuffery, S., Hamel, C., Bareil, C., Arnaud, B., Demaille, J., & Claustres, M. (1997). The protein truncation test (PTT) as a method of detection for choroideremia mutations. *Experimental Eye Research*, *65*, 849–854. https://doi.org/10.1006/exer.1997.0392

Cartegni, L., Wang, J., Zhu, Z., Zhang, M. Q., & Krainer, A. R. (2003). ESEfinder: A web resource to identify exonic splicing enhancers. *Nucleic Acids Research*, *31*, 3568–3571. https://doi.org/10.1093/nar/gkg616

Chabot, B., & Shkreta, L. (2016). Defective control of pre-messenger RNA splicing in human disease. *Journal of Cell Biology*, *212*, 13–27. https://doi.org/10.1083/jcb.201510032

Coussa, R. G., Kim, J., & Traboulsi, E. I. (2012). Choroideremia: effect of age on visual acuity in patients and female carriers. *Ophthalmic Genetics*, *33*, 66–73. https://doi.org/10.3109/13816810.2011.623261

Cremers, F. P., Armstrong, S. A., Seabra, M. C., Brown, M. S., & Goldstein, J. L. (1994). REP-2, a Rab escort protein encoded by

the choroideremia-like gene. *Journal of Biological Chemistry*, *269*, 2111–2117.

Daguenet, E., Dujardin, G., & Valcárcel, J. (2015). The pathogenicity of splicing defects: mechanistic insights into pre-mRNA processing inform novel therapeutic approaches. *EMBO Reports*, *16*, 1640–1655. https://doi.org/10.15252/embr.201541116

den Dunnen, J. T., Dalgleish, R., Maglott, D. R., Hart, R. K., Greenblatt, M. S., McGowan-Jordan, J., … Taschner, P. E. (2016). HGVS Recommendations for the Description of Sequence Variants: 2016 Update. *Human Mutations*, *37*, 564–569. https://doi.org/10.1002/humu.22981

Desmet, F. O., Hamroun, D., Lalande, M., Collod-Beroud, G., Claustres, M., & Beroud, C. (2009). Human Splicing Finder: an online bioinformatics tool to predict splicing signals. *Nucleic Acids Research*, *37*, e67. https://doi.org/10.1093/nar/gkp215

Di Iorio, V., Esposito, G., De Falco, F., Boccia, R., Fioretti, T., Colucci, R., … Testa, F. (2019). CHM/REP1 transcript expression and loss of visual function in patients affected by choroideremia. *Investigative Ophthalmology & Visual Science*, *60*, 1547–1555. https://doi.org/10.1167/iovs.18-25501

Di Iorio, V., Orrico, A., Esposito, G., Melillo, P., Rossi, S., Sbordone, S., … Simonelli, F. (2019). Association between genotype and disease progression in Italian Stargardt patients: A Retrospective Natural History Study. *Retina.*, *39*, 1399–1409. https://doi.org/10.1097/IAE.0000000000002151

Dimopoulos, I. S., Radziwon, A., St Laurent, C. D., & MacDonald, I. M. (2017). Choroideremia. *Current Opinion in Ophthalmology*, *28*, 410–415. https://doi.org/10.1097/ICU.0000000000000392

Esposito, G., De Falco, F., Tinto, N., Testa, F., Vitagliano, L., Tandurella, I. C., … Salvatore, F. (2011). Comprehensive mutation analysis (20 families) of the choroideremia gene reveals a missense variant that prevents the binding of REP1 with Rab geranylgeranyl transferase. *Human Mutation*, *32*, 1460–1469. https://doi.org/10.1002/humu.21591

Esposito, G., Testa, F., Zacchia, M., Crispo, A. A., Di Iorio, V., Capolongo, G., … Salvatore, F. (2017). Genetic characterization of Italian patients with Bardet-Biedl syndrome and correlation to ocular, renal and audio-vestibular phenotype: Identification of eleven novel pathogenic sequence variants. *BMC Medical Genetics*, *18*, 10. https://doi.org/10.1186/s12881-017-0372-0

Fry, L. E., Patrício, M. I., Williams, J., Aylward, J. W., Hewitt, H., Clouston, P., … MacLaren, R. E. (2019). Association of messenger RNA level with phenotype in patients with choroideremia: Potential implications for gene therapy dose. *JAMA Ophthalmology*, *138*, 128–135. https://doi.org/10.1001/jamaophthalmol.2019.5071

Furgoch, M. J., Mewes-Arès, J., Radziwon, A., & Macdonald, I. M. (2014). Molecular genetic diagnostic techniques in choroideremia. *Molecular Vision*, *20*, 535–44. PMCID:PMC4000712.

Garanto, A., van der Velde-Visser, S. D., Cremers, F. P. M., & Collin, R. W. J. (2018). Antisense oligonucleotide-based splice correction of a deep-intronic mutation in CHM underlying choroideremia. *Advances in Experimental Medicine and Biology*, *1074*, 83–89. https://doi.org/10.1007/978-3-319-75402-4_11

Garcia-Lopez, A., Tessaro, F., Jonker, H. R. A., Wacker, A., Richter, C., Comte, A., … Scapozza, L. (2018). Targeting RNA structure in SMN2 reverses spinal muscular atrophy molecular phenotypes. *Nature Communications*, *9*, 2032. https://doi.org/10.1038/s41467-018-04110-1

Gruber, A. R., Bernhart, S. H., & Lorenz, R. (2015). The ViennaRNA web services. *Methods in Molecular Biology*, *1269*, 307–326. https://doi.org/10.1007/978-1-4939-2291-8_19

Hamasaki-Katagiri, N., Lin, B. C., Simon, J., Hunt, R. C., Schiller, T., Russek-Cohen, E., … Kimchi-Sarfaty, C. (2017). The importance of mRNA structure in determining the pathogenicity of synonymous and non-synonymous mutations in haemophilia. *Haemophilia*, *23*, e8–e17. https://doi.org/10.1111/hae.13107

Jauregui, R., Park, K. S., Tanaka, A. J., Cho, A., Paavo, M., Zernant, J., … Tsang, S. H. (2019). Spectrum of disease severity and phenotype in choroideremia carriers. *American Journal of Ophthalmology*, *207*, 77–86. https://doi.org/10.1016/j.ajo.2019.06.002

Liu, W., Zhou, Y., Hu, Z., Sun, T., Denise, A., Fu, X. D., & Zhang, Y. (2010). Regulation of splicing enhancer activities by RNA secondary structures. *FEBS Letters*, *584*, 4401–4407. https://doi.org/10.1016/j.febslet.2010.09.039

Long, J. C., & Caceres, J. F. (2009). The SR protein family of splicing factors: master regulators of gene expression. *Biochemical Journal*, *417*, 15–27. https://doi.org/10.1042/BJ20081501

Matera, A. G., & Wang, Z. (2014). A day in the life of the spliceosome. *Nature Reviews Molecular Cell Biology*, *15*, 108–121. https://doi.org/10.1038/nrm3742

Mitsios, A., Dubis, A. M., & Moosajee, M. (2018). Choroideremia: From genetic and clinical phenotyping to gene therapy and future treatments. *Therapeutic Advances in Ophthalmology*, *10*, 2515841418817490. https://doi.org/10.1177/2515841418817490

Murro, V., Murro, V., Mucciolo, D. P., Passerini, I., Palchetti, S., Sodi, A., … Rizzo, S. (2017). Retinal dystrophy and subretinal drusenoid deposits in female choroideremia carriers. *Graefe's Archive for Clinical and Experimental Ophthalmology*, *255*, 2099–2111. https://doi.org/10.1007/s00417-017-3751-5

Radziwon, A., Arno, G., Wheaton, K. D., McDonagh, E. M., Baple, E. L., Webb-Jones, K., … MacDonald, I. M. (2017). Single-base substitutions in the CHM promoter as a cause of choroideremia. *Human Mutation*, *38*, 704–715. https://doi.org/10.1002/humu.23212

Rak, A., Pylypenko, O., Niculae, A., Goody, R. S., & Alexandrov, K. (2003). Crystallization and preliminary X-ray diffraction analysis of monoprenylated Rab7 GTPase in complex with Rab escort protein 1. *Journal of Structural Biology*, *141*, 93–95. https://doi.org/10.1016/s1047-8477(02)00634-2

Sanchez-Alcudia, R., Garcia-Hoyos, M., Lopez-Martinez, M. A., Sanchez-Bolivar, N., Zurita, O., Gimenez, A., … Ayuso, C. (2016). A comprehensive analysis of choroideremia: From genetic characterization to clinical practice. *PLoS One*, *11*, e0151943. https://doi.org/10.1371/journal.pone.0151943

Sankila, E. M., Tolvanen, R., van den Hurk, J. A., Cremers, F. P., & de la Chapelle, A. (1992). Aberrant splicing of the CHM gene is a significant cause of choroideremia. *Nature Genetics*, *1*, 109–113. https://doi.org/10.1038/ng0592-109

Schwarz, J. M., Cooper, D. N., Schuelke, M., & Seelow, D. (2014). MutationTaster2: Mutation prediction for the deep-sequencing age. *Nature Methods*, *11*, 361–362. https://doi.org/10.1038/nmeth.2890

Sengillo, J. D., Lee, W., Bakhoum, M. F., Cho, G. Y., Chiang, J. P., & Tsang, S. H. (2018). Choroideremia associated with a novel synonymous mutation in gene encoding REP-1. *Retinal Cases & Brief Reports*, *12*, 67–71. https://doi.org/10.1097/ICB.0000000000000647

Simunovic, M. P., Jolly, J. K., Xue, K., Edwards, T. L., Groppe, M., Downes, S. M., & MacLaren, R. E. (2016). The spectrum of CHM gene mutations in choroideremia and their relationship to

clinical phenotype. *Investigative Ophthalmology & Visual Science*, *57*, 6033–6039. https://doi.org/10.1167/iovs.16-20230

Singh, R. N., & Singh, N. N. (2018). Mechanism of splicing regulation of spinal muscular atrophy genes. *Advances in Neurobiology*, *20*, 31–61. https://doi.org/10.1007/978-3-319-89689-2_2

Soemedi, R., Cygan, K. J., Rhine, C. L., Glidden, D. T., Taggart, A. J., Lin, C. L., … Fairbrother, W. G. (2017). The effects of structure on pre-mRNA processing and stability. *Methods*, *125*, 36–44. https://doi.org/10.1016/j.ymeth.2017.06.001

Trapani, I., & Auricchio, A. (2019). Has retinal gene therapy come of age? From bench to bedside and back to bench. *Human Molecular Genetics*, *28*, R108–R118. https://doi.org/10.1093/hmg/ddz130

Vaché, C., Torriano, S., Faugère, V., Erkilic, N., Baux, D., Garcia-Garcia, G., … Roux, A. F. (2019). Pathogenicity of novel atypical variants leading to choroideremia as determined by functional analyses. *Human Mutation*, *40*, 31–35. https://doi.org/10.1002/humu.23671

van den Hurk, J. A., van de Pol, D. J., Wissinger, B., van Driel, M. A., Hoefsloot, L. H., de Wijs, I. J., … Cremers, F. P. (2003). Novel types of mutation in the choroideremia (CHM) gene: A full-length L1 insertion and an intronic mutation activating a cryptic exon. *Human Genetics*, *113*, 268–275. https://doi.org/10.1007/s00439-003-0970-0

Warf, M. B., & Berglund, J. A. (2010). Role of RNA structure in regulating pre-mRNA splicing. *Trends in Biochemical Sciences*, *35*, 169–178. https://doi.org/10.1016/j.tibs.2009.10.004

Wu, J. Y., & Maniatis, T. (1993). Specific interactions between proteins implicated in splice site selection and regulated alternative splicing. *Cell*, *75*, 1061–1070. https://doi.org/10.1016/0092-8674(93)90316-i

Yadegari, H., Biswas, A., Akhter, M. S., Driesen, J., Ivaskevicius, V., Marquardt, N., & Oldenburg, J. (2016). Intron retention resulting from a silent mutation in the VWF gene that structurally influences the 5' splice site. *Blood*, *128*, 2144–2152. https://doi.org/10.1182/blood-2016-02-699686

Zhou, Q., Yao, F., Han, X., Li, H., Yang, L., & Sui, R. (2017). Rep1 copy number variation is an important genetic cause of choroideremia in Chinese patients. *Experimental Eye Research*, *164*, 64–73. https://doi.org/10.1016/j.exer.2017.07.016

Zuker, M. (2003). Mfold web server for nucleic acid folding and hybridization prediction. *Nucleic Acids Research*, *31*, 3406–3415. https://doi.org/10.1093/nar/gkg595

SUPPORTING INFORMATION

Additional supporting information may be found online in the Supporting Information section.

Fig S1-S4

How to cite this article: Fioretti T, Ungari S, Savarese M, et al. A putative frameshift variant in the *CHM* gene is associated with an unexpected splicing alteration in a choroideremia patient. *Molecular Genetics & Genomic Medicine*. 2020;8:e1490. https://doi.org/10.1002/mgg3.1490